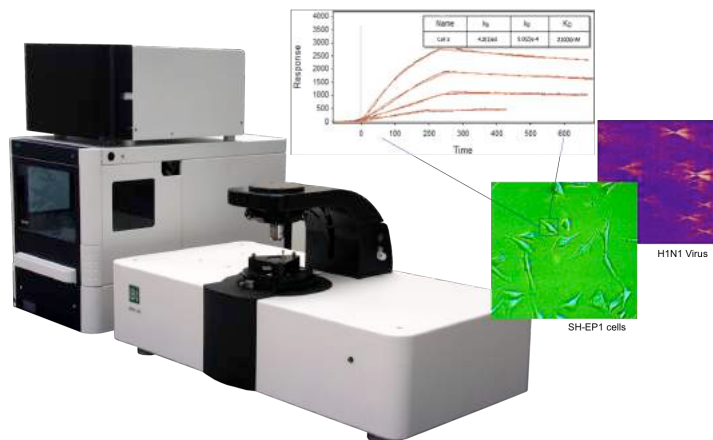


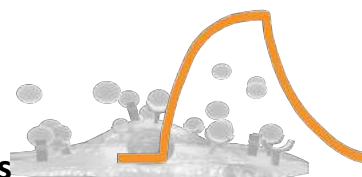
SPRm 200 Series



*Integrated optical microscopy with SPR
Label-free whole-cell SPR assays*

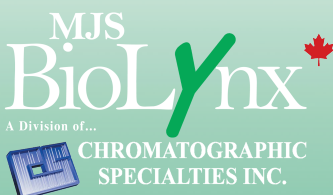


- ✧ Label-free molecular binding measurement of *in vitro* cell membrane proteins
- ✧ Quantitative mapping of binding affinity and kinetics in real time
- ✧ Simultaneous optical imaging with SPR measurements
- ✧ Direct drug interaction studies of multiple and single cells
- ✧ Nanoscale monitoring of virus and bacteria binding events



The award winning SPRm 200 system opens a new frontier in the study of molecular interactions by integrating optical microscopy with Surface Plasmon Resonance technology. Designed especially for *in-vitro*, label-free measurement of binding activity and cell kinetics, SPRm 200 provides a spatial visualization of cellular structures together with local binding activities. Real-time interactions of the drug and membrane protein can be measured in its native state without needing to extract proteins from the cell. With its outstanding sensitivity and stability, SPRm 200 also measures binding activities of bacteria and virus interactions and enables development of new methods for nanoparticle drug delivery.

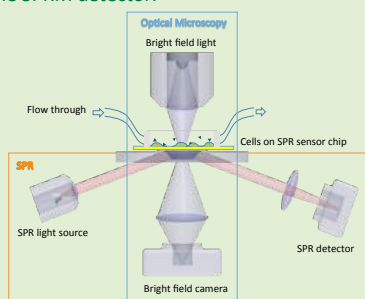
Available in Canada from...



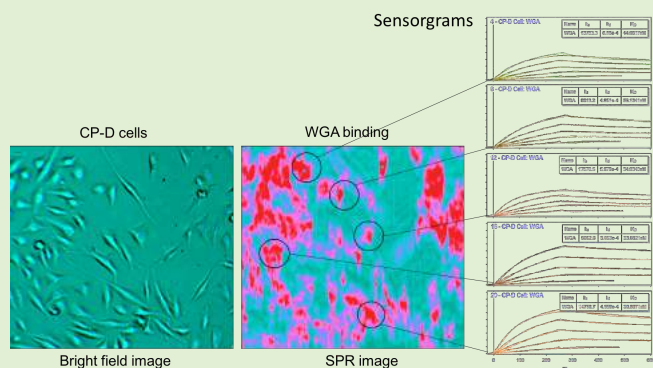
1-888-593-5969 • biolynx.ca • tech@chromspec.com

Integration of SPR with optical microscopy

Surface Plasmon Resonance Microscopy (SPRM) combines optical imaging with SPR technology, providing spatial mapping of the binding activity on living cells. A light condenser illuminates the cell grown on the sensor surface, and the optical microscope camera captures the bright field image of the cells. Simultaneously, the SPR light source projects a beam at its resonance angle onto the sensor and the reflected beam is collected by the SPRM detector.



The detector measures the SPR response at each pixel and maps them into a SPR image. At every pixel, a sensorgram is recorded, thus providing much more localized information. SPRM makes it possible to study heterogeneous surface binding and interactions of membrane proteins in their native states.

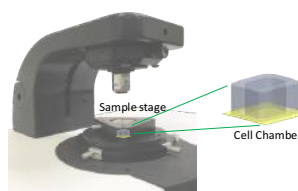


Simultaneous images of bright field (left) and SPR (middle) of Live Barrett's esophagus-derived CP-D cells binding to glycoprotein receptors. Sensorgrams of selected cells on the right.

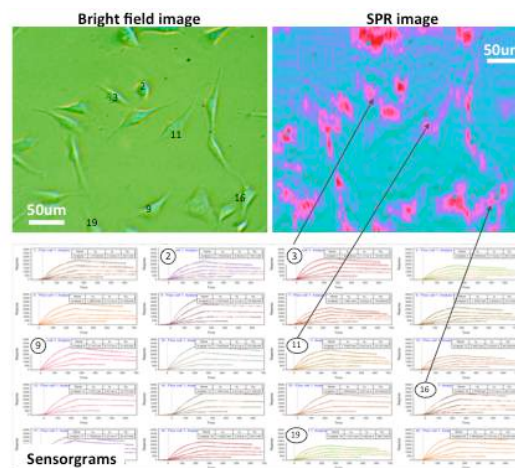
Lectin-Glycoprotein interactions

Basic cellular and therapeutic processes usually start with the binding of ligands to membrane proteins, and the study of the binding activities of membrane proteins in their native states is critical to the understanding of their biological functions.

Binding studies of the cell-surface glycosylation of SH-EP1 human epithelial cells were done with lectins (WGA, wheat-germ agglutinin). The exposure of WGA to the cells resulted in a local increase of SPR, which indicates the presence of these sugar residues on the glycan chains of the membrane proteins where the lectins are bound.



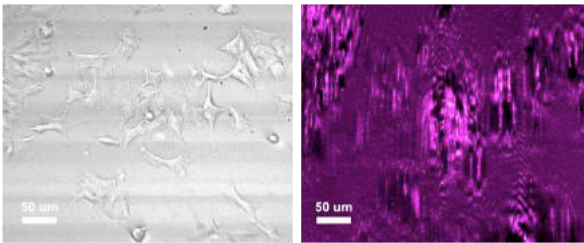
SH-EP1 cells were incubated in the cell chamber on the sensor surface and sensorgrams were recorded at each pixel. By averaging the pixel within the cell image, the binding kinetics for each cell was derived.



Bright field image of SH-EP1 human epithelial cells (top left). SPR image of lectin proteins binding to glycoprotein receptors on cells (top right). Sensorgrams of selected 20 cells shown. $k_a=4.3 \times 10^3 \text{ M}^{-1}\text{s}^{-1}$, $k_d=1.1 \times 10^{-3} \text{ s}^{-1}$ and $KD=257 \text{ nM}$.

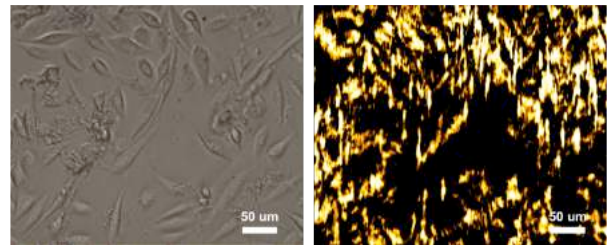
Selected SPRM Publications

1. J Lu, Y Wang, W Wang, J Li, NJ Tao, S Wang, "Label-free Imaging of Histamine Mediated G Protein-Coupled Receptors Activation in Live Cells", *Analytical Chemistry*, 88, 11498-11503, 2016
2. K Syal, R Iriya, Y Yang, H Yu, S Wang, S Haydel, HY Chen, NJ Tao, "Antimicrobial Susceptibility Test with Plasmonic Imaging and Tracking of Single Bacterial Motions on Nanometer Scale", *ACS Nano*, 10, 845-852, 2016
3. F Zhang, S Wang, L Yin, Y Yang, Y Guan, W Wang, H Xu, NJ Tao, "Quantification of Epidermal Growth Factor Receptor Expression Level and Binding Kinetics on Cell Surfaces by Surface Plasmon Resonance Imaging", *Analytical Chemistry*, 87(19), 9960-9965, 2015
4. L Yin, W Wang, S Wang, F Zhang, S Zhang, NJ Tao, "Measuring Binding Kinetics of Antibody-Conjugated Gold Nanoparticles with Intact Cells", *Small*, 2015
5. W Wang, L Yin, L G-M, S Wang, X Yu, S Eaton, S Zhang, H Chen, J LaBaer, NJ Tao, "In situ drug-receptor binding kinetics in single cells: a quantitative label-free study of anti-tumor drug resistance", *Scientific Reports*, 4, 1-7, 2014
6. W Wang, Y Yang, S Wang, V Nagaraj, Q Liu, J Wu and NJ Tao, "Label-free measuring and mapping of binding kinetics of membrane proteins in single living cells", *Nature Chemistry*, 4, 846-853, 2012
7. S Wang, X Shan, U Patel, X Huang, J Lu, J Li and NJ Tao, "Label-free imaging, detection, and mass measurement of single viruses by surface plasmon resonance." *Proceedings of the National Academy of Sciences* 107.37, 16028-16032, 2010



Peptide interactions on A549 cells

Bright field image of A549 adenocarcinomic human alveolar basal epithelial cells (left). SPR image of 8 kDa Affibody peptide binding on cells (right). $k_a=7.1 \times 10^4 \text{ M}^{-1}\text{s}^{-1}$, $k_d=7.2 \times 10^{-3} \text{ s}^{-1}$ and $K_D=10.2 \text{ nM}$.

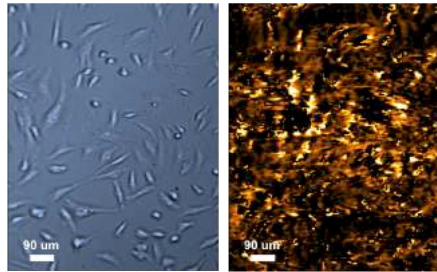


Live CP-D cells interaction

SPR image of Live Barrett's esophagus-derived CP-D (CP-18821) cells binding with WGA, a lectin that can recognize *N*-acetylglucosamine (GlcNAc). $K_D=38.7 \text{ nM}$.

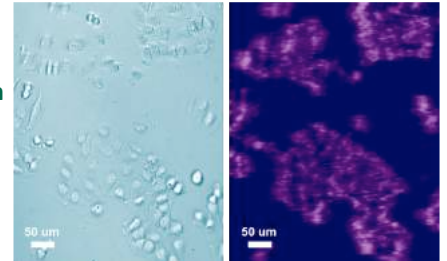
WGA interactions with CHO cells

Bright field image of CHO (Chinese hamster ovary) cells (left). SPR image of lectins binding to cells (right). $k_a=4.8 \times 10^5 \text{ M}^{-1}\text{s}^{-1}$, $k_d=2.7 \times 10^{-3} \text{ s}^{-1}$ and $K_D=5.68 \text{ nM}$.



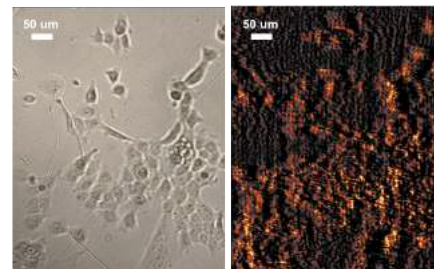
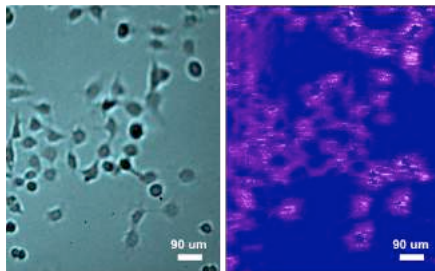
Mapping antibody binding of H4 human neuroglioma cells

Bright field image of H4 cells (left). SPR image of antibody binding to H4 cells (right). $K_D=16.8 \text{ nM}$.



GPCR interaction of HEK 293A cells

HEK 293A cell bright field image (left) and GPCR binding interaction with a 500 Da small molecule drug (right). $K_D=7.41 \text{ nM}$.

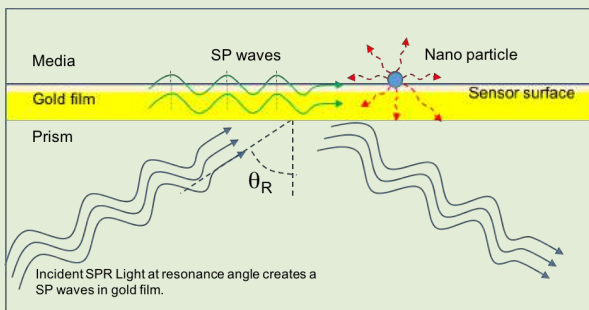


EGFR binding affinity on A431 cells

SPR image of monoclonal anti-EGFR interactions with EGFR over expressed A431 human epidermal cells. $K_D=371 \text{ pM}$.

Nanoparticle detection

SPR light projected onto the sensor at its resonance angle creates a propagating surface plasmonic (SP) waves along the metal film surface. When a nanoparticle binds to the sensor surface, it acts as a scattering center in the SP waves, creating a wake pattern with a footprint up to 100X than its actual size. This enlarged footprint enables the detection of particles smaller than the optical diffraction limit, allowing nanometer scale binding activities be monitored and studied by measuring and mapping these footprints.

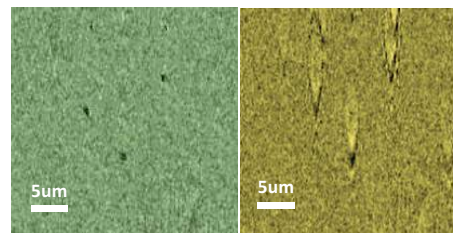


SPR image

The occurrence and intensity changes of the wake patterns in the SPR image provide rich information about binding events between the sensor surface and the nanoparticles, as well as their interactions with other molecules in the media [2,7].

Bacteria and Antibiotics

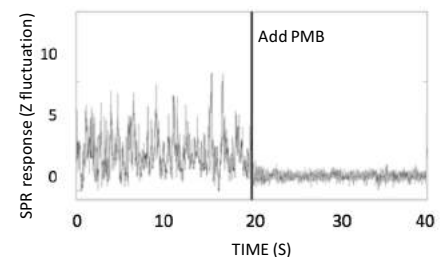
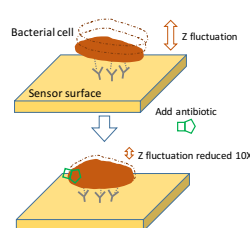
The live *E. coli* O157:H7 cells are tethered on a sensor chip via antibody coupling in a Luria Broth culture medium. They scatter the propagating SP waves creating wake patterns in the SPR image.



Bright field image

SPR image

While the bright field image of the bacterial cell (black dots) appears to be constant, the contrast of wake pattern in the SPR image fluctuates significantly.



The fluctuation, caused by the bacterial cell nanomotion provides insight into its metabolism. When bactericidal antibiotic (PMB) is added into the cell chamber, the fluctuation of the bacterial cell reduces drastically, thus revealing lethality [2].

SPRm 200 Specifications

Base Station	Light source	690 nm
	Incident angles	40-76 Deg (continuous)
	Baseline noise	< 0.6 RU RMS (0.1 mDeg RMS)
	Baseline drift	3 RU/hr (0.5 mDeg/hr) (when ambient drifts < 1°C/hr)
	Temperature Control Range	15°C to 40°C (10°C below ambient temperature max)
	Field of view	Bright Field: 1200 x 900 μ m SPR: 600 x 450 μ m
	Magnification	Bright Field: x10 SPR: x20
	Resolution	Bright Field & SPR: 1 μ m
	Stage translation / rotation	3mm x 3mm / 360 deg
	Outer dimension	690 (w) x 330 (h) x 340 (d) mm
	Weight	23 kg
	Power supply	110-230 V 50/60 Hz
Fluid Handling	Sample volume	1 to 1500 μ L (application dependent)
	Kinetic constant	$k_a < 1 \times 10^7 \text{ M}^{-1} \text{ s}^{-1}$ $k_d > 1 \times 10^{-5} \text{ s}^{-1}$
	Dissociation constant	$K_D = 10^{-3} \text{ M}$ (1 mM) to 10^{-12} M (1 pM)
	Molecular weight cutoff	200 Da
Control System	Computer	Windows operating system
	Software	ImageSPR™ software including Data Analysis and Kinetics Analysis
Autosampler (option)	Sample capacity	2 x SBS standards (384 / 96), 2 x 48 Vials (1.5mL), 2 x 12 Vials (10mL)
	Sample cooling	Minimum: 4°C +/- 2°C
	Outer dimension	300 (w) x 575 (h) x 360 (d) mm
	Weight	21 kg
Automatic Buffer Exchange Pump and Degasser (option)	Buffer exchange	Automatic buffer exchange up to six sources
	Buffer degasser	In-line
	Buffer delivery	Continuous
	Outer dimension	305 (w) x 191 (h) x 330 (d) mm
	Weight	6.8 kg

Sensors and consumables

Gold Sensor Chip

Highly uniform gold film for reproducible SPR research.



Cell chamber kit

Gold sensor chip with a silicone well for growing cells; includes chemicals and other accessories for treating sensor surfaces.



QR for Website

Email: Info2BI@BiosensingUSA.com

Website: www.BiosensingUSA.com

Tel: 1-480-491-2777 Fax: 1-866-897-8741